GEOCHRONOMETRIA 48 (2021): 16–30
Research article • DOI 10.2478/geochr-2021-0002

sciendo

Available online at
https://content.sciendo.com/view/journals/geochr/geochr-overview.xml

REVISION OF THE HUMAN'S OCCUPATIONS CHRONOLOGIES AT THE SENEGALESE AND MAURITANIA SITES BY USING MARINE RESERVOIR AGES CORRECTIONS

MAURICE NDEYE[1,*], DEMBA KEBE[2], MATAR SENE[3], ADAMA HAROUNA ATHIE[2]

[1] *Laboratoire Carbone 14, IFAN Ch.A.Diop, Cheikh Anta Diop, University Dakar, Sénégal*
[2] *Laboratoire d'Archéologie, IFAN Ch.A.Diop, Cheikh Anta Diop University Dakar, Sénégal*
[3] ***Département de physique, Faculté des Sciences et de Technologies, Cheikh Anta Diop University Dakar, Sénégal***

Received 19 May 2020 Accepted 08 February 2021

Abstract
The prehistoric settlement of the west coast of the Senegalese-Mauritanian basin is established from archaeological remains and coal samples collected, sometimes in a stratigraphic context. However, the chronology issued, in the Before Present (BP) age, does not take into account the taphonomic context of the sites and the local reservoir age. Therefore, this article revisits the chronologies obtained based on the ^{14}C literature and dating(s) acquired. Changes in time and duration of human occupancy of the area are shorter or longer depending on adequate yields of local reservoir age (Ndeye, 2008), which is a relevant element for marine samples. Thus, the archaeological implications observed with the reservoir effect are the rejuvenation or ageing of the dates, the age of the sites, the duration of occupation prehistoric or historical sites studied. Using the calibration programmes, it is noted that for the site of Senegal (Khant), without taking into account the reservoir effect, the human occupation is a priori, from the fifth millennium (Ancient Neolithic) to the third millennium BC (Middle Neolithic). However, if this marine reservoir effect is applied, the chronological periodisation goes from the fourth millennium to the first millennium. For the Mauritanian sites, the reservoir age correction is necessary for the Chami site while for the Tintan site is not required. Therefore, the calibrated archaeological chronologies obtained after the application of the marine reservoir effect are more relevant.

Keywords
marine reservoir age, calibration, marine organism, kjokkemmoddings (shell clusters)

1. Introduction

The use of ^{14}C ages from samples that grow in marine environments (i.e. molluscs, fish bones, etc.) requires special consideration like calibration, which is important for interpreting or comparing historical or climatic records. Mixing of water masses (i.e. during upwelling) may dilute the amount of ^{14}C in the water. Marine organisms that absorb their carbon from dissolved inorganic carbon (DIC) typically have relatively older ages due to the dilution effect in the ocean, as compared to atmospheric ages. Models of exchange between the atmosphere and the ocean have been proposed for surface waters (0–75 m), thermocline waters (75–1000 m) and deep waters (1000–3800 m) (Stuiver and Braziunas, 1993). From the model of surface waters, verified by ^{14}C dates on shells of known ages, one can calculate a global mean value for pre-AD 1950 marine reservoir age correction R(t) of 400 years. Some laboratories publish ^{14}C ages without reservoir effect corrections; however, this approximation is not sufficient for archaeological applications that require calibration using programs such as CALIB7.1 (Stuiver *et al*., 2013) or CALIB8.2 (Heaton *et al*., 2020).

Corresponding author: M. Ndeye
e-mail: maurice.ndeye@ucad.edu.sn

ISSN 1897-1695 (online), 1733-8387 (print)

It has been demonstrated that the variability of reservoir ages at a particular site depends on oceanic water mass circulation and mixing (Siani *et al*., 2000; Southon *et al*., 2002). In upwelling zones, for instance, mixing of deep waters with surface waters produces important local reservoir effects, with ΔR values of several hundred years or more. Previous studies (Ndeye, 2008) focussed on the estimation of the mean value for the reservoir effect for coastal Senegal and Mauritania, western Africa. It has been suggested that the reservoir effect in this part of Africa could be high because it should be affected by upwelling phenomena (Goodfriend and Flessa 1997). That study area extends from Port Etiénne (21° 01′N, 17° 02′W) (coastal Mauritania) in the north to Rufisque (14° 42′N, 17° 15′W) on the Cap-Vert (Cape Verde) peninsula (coastal Senegal). ^{14}C dates were calculated from AD 1837 and 1945 using gastropods from which are calculated reservoir ages. The weighted mean results of R for Senegal is 511 ± 50 Before Present (BP) and ΔR is 176 ± 15 BP; for Mauritania, R is 421 ± 15 BP and ΔR is 71 ± 13 BP. The stations studied are part of the family-face distribution of archaeological sites in the West African Neolithic. From this classification and dating, the settlement of Khant, Chami and Tintan stretches from the ancient Neolithic to the historical period. However, the problem of these chronologies, with periods of hiatus, is the consideration of the influence of the marine effect on the samples collected. Hence, the question of the absolute accuracy of the dates obtained. From the BP age classification, the sites are ‘old’ and the chrono-cultural and taphonomic conceptuality of the stations are poorly defined. Therefore, the application of the local reservoir effect allows greater consistency in the ‘timing’ of the calibrated samples and occupancy. This article aims to provide revisited chronology of two human settlements in Mauritania and Senegal, applying the age characteristics of the reservoirs previously published from the Mauritanian and Senegalese coast.

2. Material and Methods

2.1. Description of the Studied Sites and excavations

2.1.1. Khant site (Senegal)

Ravisé discovered the site of Khant in 1968. It is a depression located at 22 km (16°04′02.8″N; 16°20′25.7″W) of the city of Saint-Louis (Fig. 1). Human occupation of the coastline at the beginning of the Holocene is facilitated by the availability of coastal resources (molluscs, fish and marine mammals). This is the archaeological essence (shellfish) of

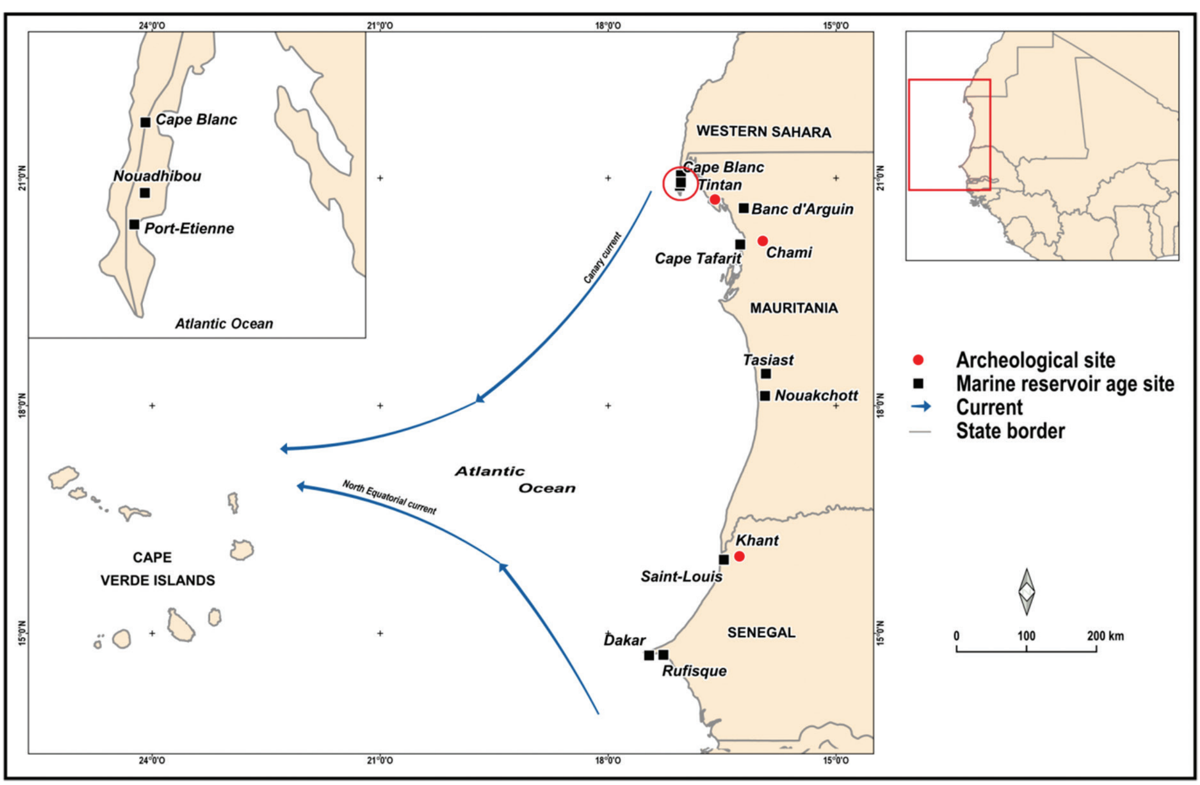

Fig 1. Sampling sites for reservoir ages calculations and the studied archaeological sites.

the Khant site (excavated in 1970 by Ravisé) whose duration of occupation begins between 5650 ± 140 BP (Ly 990) and 5248 ± 177 PB (Ravisé *et al.*, 1975; Hebrard, 1978). Similarly, radiocarbon dating on Anadara Senilis shells of 5340 ± 120 BP (Ly 988), 4352 ± 123 BP (Dk60) and 4225 ± 119 BP (Dk69) were obtained. In addition, a charcoal sample, taken at a depth of 150 cm (Ravisé, id.) is dated at 1751 ± 13 BP.

Other dates obtained in the vicinity of the Khant depression, despite the inaccuracy of their location, range from 5000 BP to 1500 BP (Table 1; Mbow 1987). On this site remains of burials of a Negroid type subject have been reported. Therefore, based on calibrated ages (Ravisé *et al.*, 1975), the settlement of Khant stretches from the ancient Neolithic to the protohistorical era (1000 BC to 1500 AD).

The Khant site has delivered polished bone axes, harpoons, hooks and ceramics whose properties match those of the Atlantic coast' (Ravisé, 1970). The ground shell and its derivatives were used as technical elements (tool shaping) and as a basis for dating the site.

2.1.2. Tintan and Chami sites (Mauritania)

Tintan and Chami integrate into the entire Mauritanian coast (Fig. 1). These two sites have affinities with Khant in Senegal. In the seventh millennium, human occupation affected part of the coastline. From the fifth and fourth millennia, the coast, entirely occupied, encompasses Tintan and Chami. Tintan and Chami integrate into the entire Mauritanian coast. Traces of prehistoric settlement (epipaleolithic and neolithic) are found in the area of Foum Arguin, in Chami but novelties, heralds of the Neolithic make their appearance—arrow frames, often bifacial, polished axes, ceramics, grinding equipment (Vernet, 2004). The Tintan site, on the Tintan peninsula, is 7 km from Foum Arguin, north of Banc d'Arguin. It is part of the Senegalese-Mauritanian coastal strip from Saint-Louis to Nouadhibou. Tintan is limited to the north, from Cap Blanc, by Nouadhibou-Cansado, the Banc d'Arguin to the south, to the East Foum Arguin and to the West the Atlantic coast. Tintan, 'older', like Khant are Neolithic stations. Thus, the dating obtained in this region, by J.P. Charbonnel are in the intervals from 6020 ± 150 BP (on shells) to 5670 ± 300 BP (on Arca Senilis), at 4270 ± 100 BP (on cymbium) and/or 3530 ± 130 BP (on Arca Senilis). Fonte obtained a date of 4860 ± 160 BP. Thus, in the evolution of the occupation, the culture of Tintan slips into the peninsula of the same name and the Tasiast.

2.1.2.1. Chami site

Chami is a «Hasi[1]», (20° 03′03″N; 15°58′0.3″W) gateway to the Banc d'Arguin, located on the Nouadhibou-Nouakchott axis, east of Cape Tafarit. In addition, while Chami does not have a real food discharge area, there are, however, many deteriorated shells on the surface of the occupied dunes (Farida, 2013). Consequently, Petit-Maire in 1979, who searched the site, collected the following dates on cymbium: 2360 ± 100 BP, 3220 ± 110 BP, 3950 ± 80 BP. While J.P. Charbonnel collected in Chami Tafarit, on Arca Senilis 3570 ± 120 BP. Most of the population lived on the inland dunes (Chami, Tijirit, etc.). Chami is presented in the form of wind mounds specific to the dune industries that outcrop on the whole great coast from Dakar to Banc d'Arguin. As a result, the lithic industry is carved on flint. The industry is made up of flash nuclei. The tooling is composed of scrapers, collectors, scales and denticula, geometric pieces (segments, trapezes and triangles), common to the dune industries of Senegal. Arrowhead reinforcements are preferentially pedunculated (Vernet, 1993). Traces of prehistoric settlement (epipaleolithic and neolithic) are found in the area of Foum Arguin, in Chami but novelties, heralds of the Neolithic make their appearance—arrow frames, often bifacial, polished axes, ceramics, grinding equipment (Vernet, 2004). This lithic production is associated with ceramics, with many decorated shards.

[1] a well

2.1.2.2. Tintan site

The Tintan site (16°24′0″N; 10°10′0″), on the Tintan peninsula is 7 km from Foum Arguin, north of Banc d'Arguin. It is part of the Senegalese-Mauritanian coastal strip from Saint-Louis to Nouadhibou. Tintan is limited to the north, from Cap Blanc, by Nouadhibou-Cansado, the Banc d'Arguin to the south, to the East Foum Arguin and to the West the Atlantic coast. Tintan, 'older', like Khant are Neolithic stations. Thus, the radiocarbon datings obtained in this region, by J. P. Charbonnel are in the intervals 6020 ± 150 BP (on shells), 5670 ± 300 BP (on Arca Senilis), at 4270 ± 100 BP (on cymbium) and/or 3530 ± 130 BP (on Arca Senilis). JC Fontes obtained a date of 4860 ± 160 BP. Thus, in the evolution of the occupation, the culture of Tintan slips into 'peninsula of the same name and from Tasiast to the region of Chami. Further south, the Nouakchott region and the Aftout es Sahili region are attracting more and more men' (Vernet and Tous, 2004). In addition, the geological configuration of the region allows the outcropping of raw materials, of rocks suitable for size. Thus, the Tintan deposit is of great lithic wealth and collections of Senelia, which greatly contribute to the activity of specialised groups (Vernet *et al.*, 2004).

2.2. Methods

2.2.1. Literature data

We used archaeological reports (Vernet, 1998), articles (Delibrias and Evin, 1980) which allowed us to collect 18

Table 1. *Calibration of marine samples collected at the Khant, with the atmospheric curve and the Marine curves (ΔR = 0 BP or ΔR = 176 ± 15 BP or ΔR = 27 ± 56 BP).*

Sample location	Sample code	Sample type	Age (BP)	Atmospheric calibration[a] (BC/AD)	Marine calibration[b] (BC/AD) ΔR = 0 BP	Marine calibration[c] (BC/AD) ΔR = 176 ± 15 BP	Marine calibration[d] (BC/AD) ΔR = 27 ± 56 BP
Khant-1	DK-1	Anadara senelis shell	2448 ± 34	1σ: [cal BC 551: cal BC 451], 0.49 2σ: [cal BC 595: cal BC 410], 0.57	1σ: [cal BC 192: cal BC 84], 1 2σ: [cal BC 266: cal BC 29], 1	1σ: [cal AD 23: cal AD 123], 1 2σ: [cal BC 36: cal AD 169], 1	1σ: [cal BC 39: cal AD 175], 1 2σ: [cal BC 156: cal AD 265], 1
Khant4	DK-4	Anadara senelis shell	2633 ± 29	1σ: [cal BC 815: cal BC 796], 1 2σ: [cal BC 838: cal BC 783], 1	1σ: [calBC 398: cal BC 341], 1 2σ: [cal BC 466: cal BC 296], 0.97	1σ: [cal BC 200: cal BC 91], 1 2σ: [cal BC 292: cal BC 42], 1	1σ: [cal BC 279: cal BC 55], 1 2σ: [cal BC 372: cal AD 35], 1
Khant 5	DK-5	Anadara senelis shell	2663 ± 49	1σ: [cal BC 847: cal BC 797], 0.84 2σ: [cal BC 916: cal BC 782], 1	1σ: [cal BC 473: cal BC 349], 1 2σ: [cal BC 571: cal BC 246], 1	1σ: [cal BC 299: cal BC 132], 1 2σ: [cal BC 344: cal BC 56], 1	1σ[cal BC 334: cal BC 102], 1 2σ: [cal BC 410: cal AD 38], 1
Khant 7	DK-7	Anadara senelis shell	2912 ± 39	1σ: [cal BC 1131: cal BC 1041], 0.74 2σ: [cal BC 1224: cal BC 996], 1	1σ: [cal BC 792: cal BC 719], 1 2σ: [cal BC 821: cal BC 609], 0.99	1σ: [cal BC 553: cal BC 398], 1 2σ: [cal BC 664: cal BC 379], 0.98	1σ: [cal BC 633: cal BC 399], 1 2σ: [cal BC 756: cal BC 332], 1
Khant (Terrasse)	DK-69	Anadara senelis shell	4225 ± 110	1σ: [cal BC 2922: cal BC 2624], 1 2σ: [cal BC 3098: cal BC 2485], 0.99	1σ: [cal BC 2501: cal BC 2202], 0.98 2σ: [cal BC 2672: cal BC 2035], 1	1σ: [cal BC 2282: cal BC 1968], 1 2σ: [cal BC 2453: cal BC 1846], 1	1σ: [cal BC 2323: cal BC 1960], 1 2σ: [cal BC 2487: cal BC 1774], 1
Khant (Dunes)	DK-60	Anadara senelis shell	4352 ± 123	1σ: [cal BC 3119: cal BC 2878], 0.76 2σ: [cal BC 3362: cal BC 2833], 0.89	1σ: [cal BC 2740: cal BC 2387], 1 2σ: [cal BC 2865: cal BC 2214], 1	1σ: [cal BC 2466: cal BC 2129], 1 2σ: [cal BC 2634: cal BC 1943], 1	1σ: [cal BC 2501: cal BC 2113], 1 2σ: [cal BC 2698: cal BC 1916], 1
Khant (Terrasse)	DK-X	Anadara senelis shell	5040 ± 125	1σ [cal BC 4267: cal BC 3942], 0.87 2σ: [cal BC 4375: cal BC 3694], 0.98	1σ: [cal BC 3608: cal BC 3323], 1 2σ: [cal BC 3696: cal BC 3081], 1	1σ: cal BC 3358: cal BC 3022], 1 2σ: [cal BC 3509: cal BC 2888], 1	1σ: [cal BC 3362: cal BC 2996], 1 2σ: [cal BC 3538: cal BC 2840], 1
Khant (Terrasse)	DK-39	Anadara senelis shell	5248 ± 177	1σ: [cal BC 4268: cal BC 4046], 0.87 2σ: [cal BC 4406: cal BC 3946], 0.98	1σ: [cal BC 3889: cal BC 3490], 1 2σ: [cal BC 4086: cal BC 3252], 1	1σ: [cal BC 3685: cal BC 3264], 1 2σ: [cal BC 3881: cal BC 3002], 1	1σ: [cal BC 3646: cal BC 3191], 1 2σ: [cal BC 3853: cal BC 2936], 1
Khant (Terrasse)	Ly-988	Anadarasenelis shell	5340 ± 120	1σ: [cal BC 4268: cal BC 4046], 0.87 2σ: [cal BC 4464: cal BC 3975], 0.99	1 σ: [cal BC 3893: cal BC 3642], 1 2 σ: [cal BC 4020: cal BC 3507], 1	1σ: [cal BC 3697: cal BC 3438], 0.97 2σ: [cal BC 3863: cal BC 3317], 0.99	1σ[cal BC 3680: cal BC 3366], 1 2σ: [cal BC 3884: cal BC 3200], 1
Khant (Dunes)	Ly-990	Anadara senelis shell	5415 ± 120	1σ: [cal BC 4356: cal BC 4221], 0.57 1σ: [cal BC 4464: cal BC 3975], 0.99	1σ: [cal BC 3955: cal BC 3699], 1 2σ: [cal BC 4143: cal BC 3607], 1	1σ: [cal BC 3782: cal BC 3512], 1 2σ: [cal BC 3918: cal BC 3375], 1	1σ: [cal BC 3784: cal BC 3461], 1 2σ: [cal BC 3945: cal BC 3318], 1
Khant (Dunes)	DK-191	Anadara senelis shell	5650 ± 140	1σ: [cal BC 4618: cal BC 4352], 0.94 2σ: [cal BC 4836: cal BC 4232], 0.99	1σ: [cal BC 4253: cal BC 3954], 1 2σ: [cal BC 4387: cal BC 3773], 1 0	1σ: [cal BC 4044: cal BC 3720], 1 2σ: [cal BC 4230: cal BC 3624], 1	1σ: [cal BC 4037: cal BC 3680], 1 2σ: [cal BC 4230: cal BC 3529], 1

Note: The calibrated ages chosen are those with the highest probability density.

BP, Before Present.

[a]Atmospheric calibration curve: Intcal13.^{14}C (Reimer *et al*., 2013).

[b]Marine calibration curve with world marine reservoir age: Marine13.^{14}C (Reimer *et al*., 2013).

[c]Marine calibration curve with estimated marine reservoir age: Marine13.^{14}C (Reimer *et al*., 2013).

[d]Marine calibration curve with estimated marine reservoir age: Marine20.^{14}C (Heaton *et al*., 2020).

dates for Chami, 27 dates for Tintan. Radiocarbon dating was mostly carried out on marine shells in the 1980s. Only 21 dates are out of continental macrorests (Human bones; Pottery degreaser; charcoal sand).

A few rare dates were given with the corresponding isotopic fractionation $\delta^{13}C$. With regard to sea shells, the hypothesis put forward is that for $\delta^{13}C$ close to 0‰ then the correction to be applied of 400 years is compensated by the apparent age of the oceanic surface waters, which is about 400 years except in very special cases of deep water ascents.

2.2.2. Radiocarbon laboratory new data (IFAN Ch.A.Diop, Dakar)

Since 2003, a new dating system has been installed at the Carbon 14 laboratory of the IFAN Cheikh Anta Diop of the University Cheikh Anta Diop of Dakar. It is equipped with a liquid scintillation meter (Tri-carb 3170TR/LS) with BGO tube (Bi4GeO12) to reduce background noise in super low-level mode.

The performance of this dating system (background, merit factor) and the calibration were evaluated by the use of the standards of the International Atomic Energy Agency (IAEA) but also by the age known samples from the University Paris VI (France). The counter is supported by software called Quanta Smart for the Windows operating system (Packard 1999). Counting is programmed for 100 min per cycle.

In the energy range 13–85 keV, the efficiency of the meter is 68% and the background noise is 0.2 cpm. The E^2/B merit factor is 23.400. This clearly shows the high performance of the counting system. In super low-level counting mode using BGO tubes, the background noise is reduced considerably and goes down to 0.1 cpm for the same output. The newly renovated laboratory has had its first date with a new laboratory code DK.

2.2.2.1. Physical and chemical pretreatments

Before determining the age of a sample, it undergoes physicochemical pretreatments that depend not only on the nature of the sample but also on its degree of pollution. These pretreatments reduce the level of pollution. Once the samples are pretreated physically, that is, cleaned, stripped or crushed, a chemical pretreatment is usually performed in a conventional way by making acid-base-acid attacks to eliminate any pollution.

For this study, the collected marine samples are chemically pretreated. The sample is immersed in 8% HCl for about half an hour and then rinsed with swapped water. Since the sample is a shell, after a good rinse to a neutral pH, the pretreatment is completed and the sample is ready to be synthesised.

2.2.2.2. Benzene Sample Synthesis

After the pretreatments, the samples are placed in an oven at an appropriate temperature and for a time which allows to dry depending on the type of the sample. The synthesis of benzene is carried out by means of a device whose operating procedure is as follows: first of all, a primary vacuum within the synthesis bench is made, thanks to the pumps installed on the bench.

The sample is then attacked by ortho-phosphoric acid (H_3PO_4) to give carbon dioxide (CO_2). The CO_2 is sent to the lithium-containing furnace and the carburation starts at 800°C to give lithium carbide (Li_2C_2) and lithium oxide (Li_2O). Acetylene (C_2H_2) is obtained by hydrolysing the obtained lithium carbide. Finally, the trimerisation of acetylene in the presence of catalyst (vanadium–chromium) at 50°C makes it possible to obtain benzene. The benzene obtained at the end of this synthesis is put into the counting chamber of the liquid scintillation counter (Tri-carb 3170 TR/LS with BGO tube) produced by Packard in 1999, which makes it possible to obtain, after a few days (15 cycles), the activity of the sample necessary for the determination of the radiocarbon age.

2.2.2.3. Calculation of sample activity by liquid scintillation

Two grams of synthesised benzene is mixed with mixed scintillator, Bis MSB + Buthyl PBD in proportions of 6 mg each. The scintillator converts the energy of the incident particle, the β-radiation released by benzene, into photons. The incident energy carries the atoms or a molecule of the scintillator in an excited state, and their return to the ground state is accompanied by the emission of photons. These photons are received by the photocathode of the photomultipliers that emit electrons that come to hit a dynode and re-emit several electrons to another dynode.

Each time a photon reaches a dynode, it triggers a pulse or strokes. All the electrons are collected by the anode, which is the output signal of the scintillation detector. This signal is proportional to the energy released by benzene and makes it possible to determine the total number of strokes recorded over a longer or shorter period of time. The calculation of the average activity of the sample makes it possible to determine the corresponding radiocarbon age.

The radiocarbon age is calculated not only assuming the constancy of the ^{14}C content but also the consideration of isotopic fractionation (^{13}C). During the photosynthesis process, plants proportionally absorb less ^{13}C and ^{14}C isotopes than what is available in the carbon reservoir, resulting in fractionation reflected in the consumption of living beings. ^{14}C is half as absorbed as ^{13}C. Thus, the $^{12}C/^{13}C$ ratio can be used to compensate for the initial exhaustion of the ^{14}C. Radiocarbon dating must then be corrected for this isotopic fractionation: this is normalisation. Radiocarbon age is calculated using the following equation:

$$T = -8033Ln\left(\frac{A_{SN}}{A_{0N}}\right)$$

with A_{SN} and A_{0N}, respectively, the normalised sample activity at −25‰ and the normalised standard activity (Stuiver and Polach, 1977). The carbon14 half period used is 5568 years. The year 1950 is automatically used as the base age, and the ages are given in units BP, the present being the year 1950 AD (year Domini). These calculated ages take into account the isotopic fractionation corrections due to the difference in isotopic velocity in various environments.

Age calibration processes by appropriate programs such as Calib 7.04 and Calib 8.1 can then convert the radiocarbon age into real age, that is, BC units or AD units.

For the samples in this study, failing to be able to calculate the $^{12}C/^{13}C$ ratio by mass spectrometry, an isotopic fractionation correction was not made. We consider that the correction (400 years) is thus compensated by the apparent age of the surface waters. Most of the samples (DK-1 to DK-39) were analysed in the radiocarbon laboratory of IFAN Ch.A.Diop of Cheikh Anta Diop University of Dakar (Sénégal) and the rest by the Lyon dating laboratory (Ly-988, Ly-990) in France.

2.2.3. Calibration

The previously estimated reservoir ages (R) have been determined using the marine mollusc shell of historically known age from 1837 to 1945 AD (Ndeye, 2008). However, it has been demonstrated that R changes over time in response to changes in ocean circulation and climate conditions (Druffel and Griffin 1993; Dunbar and Cole 1996; Stuiver *et al*., 1986). Unfortunately, there are no published R values from archaeological (marine/terrestrial samples) in our sampling sites for the determination of the past reservoir age. The archaeological sites investigated in our study are under the NW African coastal upwelling system characterised by a complex and heterogeneous oceanographic pattern that extends south to Cape Verde in winter and north to the Iberian Peninsula in summer (Wooster *et al*., 1976; Láiz *et al*., 2000; Pelegrí *et al*., 2006). Some studies on the determination of the past reservoir age have been done in Cap Verde (Soares *et al*., 2011) using pair samples show that the reservoir age is preserved (70 ± 70 BP). Taking into account these comparisons, we applied the previously estimated modern reservoir age in the Senegalese and Mauritania archaeological sites for this study. We present the tables giving the calibrated ages for each archaeological site using three types of calibration curve (Reimer *et al.*, 2013; Heaton *et al*., 2020), and the CALIB program has been used for these calibrations. To highlight the importance of the reservoir effect, the use of chronomodel 2.0.18 (Lanos and Philippe, 2015) with the option « phase » was made for the dates of the different sites. Then, four results from the calibration curves have been obtained in this chronomodel: the phase modelling results using IntCal13; the phase modelling results using Marine13; the phase modelling results with local reservoir age applied on Marine13 and the phase modelling results using Marine20 (Heaton *et al*., 2020) with local ΔR applied.

We applied the local reservoir age of 71 ± 3 BP for Mauritanian sites and 176 ± 15 BP for Senegalese site for the marine13 calibration curves (Ndeye, 2008). These reservoir values have been recalculated and became 27 ± 56 BP and −75 ± 42 BP for Senegal and Mauritania, respectively, based on the new calibration curve Marine20 (Heaton *et al*., 2020). The duration of the phase is symbolised by the bold line, and the probability distribution of the beginning and the end of the phase is also shown.

3. Results and discussion

3.1. Khant Site (Senegal)

3.1.1. Comments 1

Looking at the four phases, we see a chronological shift towards the youngest phases. All beginnings and ends of occupation are rejuvenated. Thus, a comparison between the results of the calibration curves gives between Intcal13 and Marine13 with ΔR = 0 a difference of rejuvenation of the occupation at the beginning of 459 years. This difference is 62 years between Marine13 with ΔR = 0 and Marine13 with ΔR = 176 ± 15 BP. The comparison between Marine13 with ΔR = 176 ± 15 BP and Marine20 with ΔR = 27 ± 56 BP gives a gap of 38 years, 5119 years for Intcal13, 4660 years for Marine13 with ΔR = 0, 4598 years for Marine13 with ΔR = 176 ± 15 BP and 4560 years for Marine20.

With the Marine13 calibration curve (Fig. 2), the beginning of the human occupation of the Khant is around 4660 BC or the second half of the fifth millennium BC. Therefore, based on the established chronology, the dynamics of the establishment extends to the Khant beyond the protohistoric epoch, the beginning of history. In addition, with the application of the local reservoir age on Marine13, occupation begins in the fifth millennium BC (4598 BC), therefore a 521-year rejuvenation. The information provided by comparing the Marine13 and Marine20 calibration curves with the application of the local reservoir effect shows a 7-year rejuvenation 4044 BC to 4037

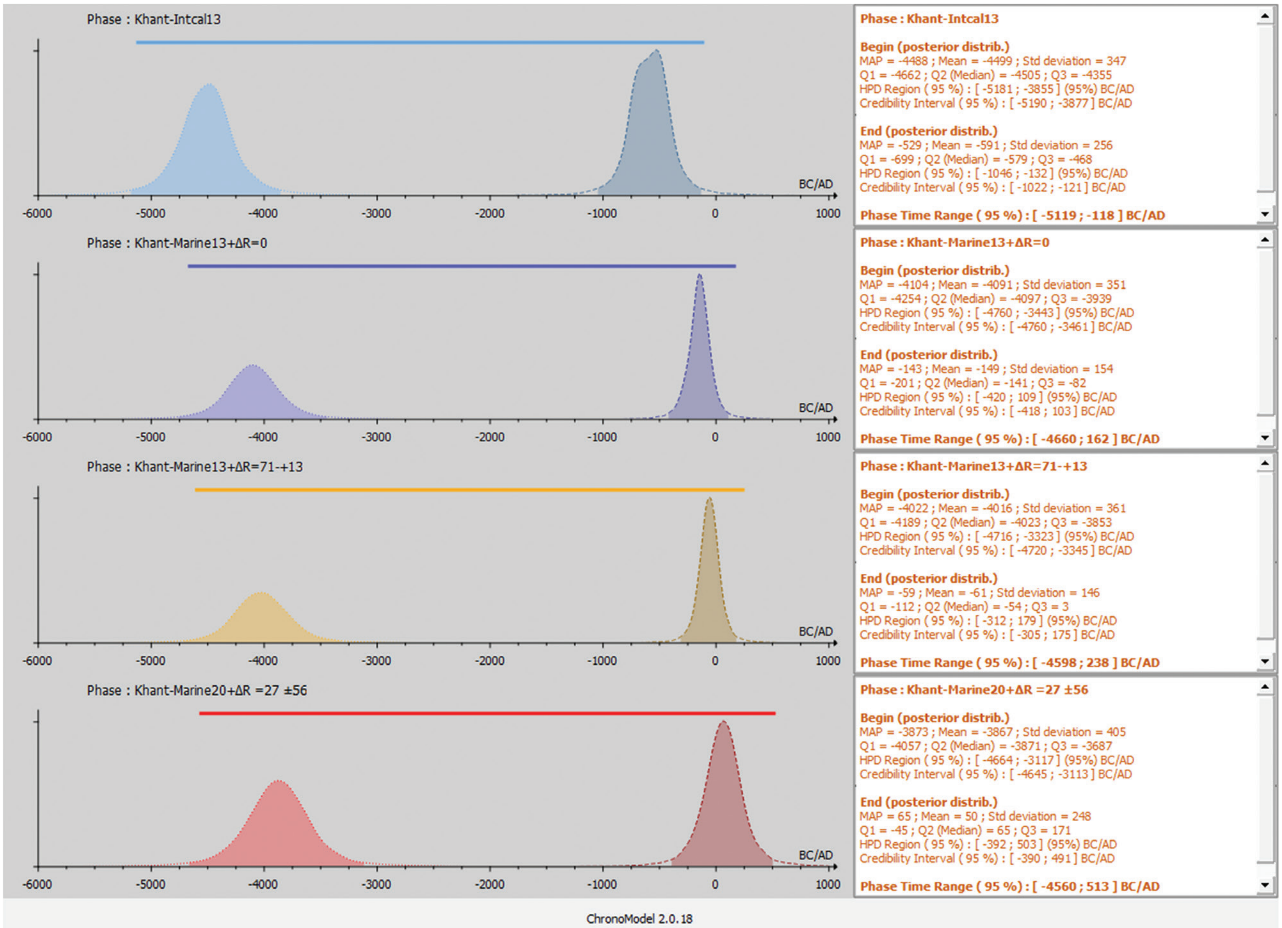

***Fig 2**. Calibration of the marine sample collected from Khant site using chronomodel 2.0.18 with phase option.*

BC (Table 1). The end of the occupation, despite a relative extension, coincided with upper, and 175 AD ageing limits on lower limits of Khant samples (238–513). In filigree, the procedural reconstruction of the Khant settlement, based on the three approaches used, shows that the occupation extends from the fifth millennium BC to the birth of the Age of Metals. In addition, the duration of occupation of Khant ranges from 5119 BC to 118 AD or from 4560 AD to 513 AD with caesura phases. The occupation is continuous since the ancient Neolithic and extends beyond the Protohistory (dates AD, early antiquity). The taphonomy of the site raises, despite the 'doubts' about the dating issued, the problem of the construction (occupation), deconstruction (abandonment) and reconstruction (reoccupation) of the Khant station.

3.2. Chami Site (Mauritania)

For the Chami, the collections of the samples were made by Petit-Maire in 1979 and the dates by the laboratories of Gif sur Yvette (France) (Gif-1856 and Gif 2524) and only one (Ly-346) by the laboratory of Lyon (France).

3.2.1. Comments 2

The first 3 phases (Intcal13, Marine13 + ΔR = 0 BP, Marine13 + ΔR = 71 ± 13 BP) show a chronological shift to the youngest phases while with Marine20 taking into account reservoir effect the phase is aged. A comparison between the results of the calibration curves gives between Intcal13 and Marine13 with ΔR = 0 gives a rejuvenation gap of the beginning of occupation of 507 years. This difference is 103 years between Marine13 with ΔR = 0 and Marine13 with ΔR = 71 ± 13 BP. The comparison between Marine13 with ΔR = 71 ± 13 BP and Marine20 with ΔR = -75 ± 42 BP gives a gap of 88 years. For the duration of the occupations, they are 2988 years for Intcal13, 2481 years for Marine13 with ΔR = 0, 2378 years for Marine13 with ΔR = 71 ± 13 BP and 2466 years for Marine20. From the Intcal13 curve to the Marine13 curve with the consideration of the reservoir effect, we have a decrease in the duration of occupancy of the site. But Marine13 with ΔR = 71 ± 13 BP, the sample ages 88 years. Nevertheless, the prehistoric occupation dynamics of the Chami at the Marine13 base ranged from 2481 to 629 AD

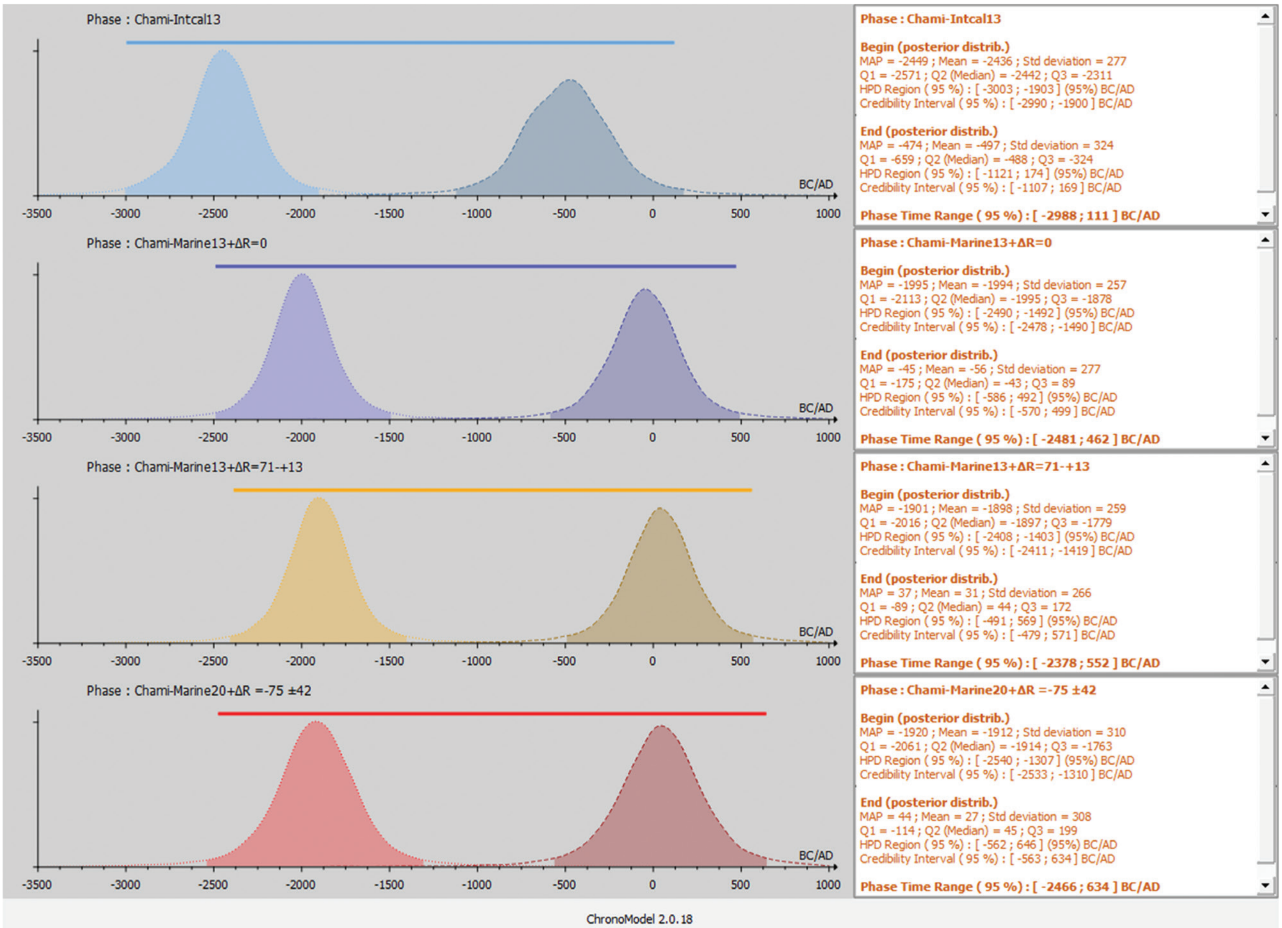

Fig 3*. Calibration of the marine sample collected from Chami site using chronomodel 2.0.18 with phase.*

(Fig. 3). The occupation extends from 2481 BC to 2378 BC the third millennium BC, while the lower limits of the dates obtained confirm the long period of settlement of Chami, from the third millennium until the beginning of antiquity, with a period of interruption Gif-2487 and Gif-2164 [930 BC–153 AD] (Table 2). The marine calibration 13 provides a beam dated between the third millennium (Middle Neolithic), hence a hiatus extending from 1500 BC to 500 BC. Hence the complexity of interpretative considerations of the curves (GIF 1856), including the chronological wasteland, in Mauritania, is the first period of the 'Protohistory' coinciding with the Bronze Age, in the West. From Ly-346 to Gif-2487, the developed culture is linked to iron metallurgy. Sample GIF-2164 is of historical age, birth of ancient 'kingdoms'. Thus, the population of the region ranges from 2481 BC to 1500 BC. From there, Chami was abandoned for more than a millennium, possibly because of the drying up of the region. From there, Chami was abandoned for more than a millennium perhaps because of the drying up of the region. The revival will occur with the rise of iron metallurgy in Africa, in 469 AD. From the lower limits, 462–629 AD, the settlement of Chami begins with the end of the Neolithic, first period of Protohistory and continues until the appearance of the first historical texts. The dates obtained by Marine13 rejuvenate Chami by just over a century: from 2481 BC to 2378 BC.

3.3. Tintan Site (Mauritania)

For the Tintane site, the excavations were made by Carbonnel in 1979 and the dating by the laboratory of Gif sur Yvette (France), Lyon (France). J.C. Fontes from the Dynamique de Paris VI geology laboratory analysed most of the samples by, but it did not adopt a laboratory code – reference 'FC' according to the inventory studies by Vernet (1998) was adopted.

3.3.1. Comments 3

For Tintan, there is also a chronological shift towards the younger phases for the first three

Table 2. *Calibration of marine samples collected at the Chami site with the atmospheric curve, and the Marine curves (ΔR = 0 BP or ΔR = 71 ± 13 BP or ΔR = -75 ± 42 BP).*

Sample location	Sample code	Sample type	Age (BP)	Atmospheric calibration[a] (BC/AD)	Marine calibration[b] (BC/AD) ΔR = 0 BP	Marine calibration[c] (BC/AD) ΔR = 71 ± 13 BP	Marine calibration[d] (BC/AD) ΔR = −75 ± 42 BP
Chami	Gif-2164	Cymbium T1	2360 ± 100	1σ: [cal BC 559: cal BC 358], 0.71 2σ: [cal BC 773: cal BC 342], 0.86	1σ: [cal BC 163: cal AD 84], 1 2σ: [cal BC 325: cal AD 190], 1	1σ: [cal BC 85: cal AD 168], 1 2σ: [cal BC 202: cal AD 315], 1	1σ: [cal BC 98: cal AD 206], 1 2σ: [cal BC 267: cal AD 350], 1
Chami	Gif-2487	Cymbium, 8	3220 ± 110	1σ: [cal BC 1632: cal BC 1391], 0.96 2σ: [cal BC 1753: cal BC 1215], 1	1σ: [cal BC 1220: cal BC 931], 1 2σ: [cal BC 1363: cal BC 824], 1	1σ: [cal BC 1122: cal BC 846], 1 2σ: [cal BC 1279: cal BC 769], 1	1σ: [cal BC 1159: cal BC 843], 1 2σ: [cal BC 1348: cal BC 740], 1
Chami-Tafarit	Gif 2524	Chells	3410 ± 110	1σ: [cal BC 1881: cal BC 1611], 1 2σ: [cal BC 1977: cal BC 1491], 0.989	1σ: [cal BC 1461: cal BC 1186], 1 2σ: [cal BC 1594: cal BC 1029], 1	1σ: [cal BC 1387: cal BC 1101], 1 2σ: [cal BC 1494: cal BC 935], 1	1σ: [cal BC 1405: cal BC 1085], 1 2σ: [cal BC 1538: cal BC 906], 1
hami	Gif-2488	Cymbium, 15 a	3450 ± 110	1σ: [cal BC 1897: cal BC 1627], 1 2σ: [cal BC 2036: cal BC 1500], 0.99	1σ: [cal BC 1501: cal BC 1228], 1 2σ: [cal BC 1640: cal BC 1077], 1	1σ: [cal BC 1425: cal BC 1144], 1 2σ: [cal BC 1553: cal BC 985], 1	1σ: [cal BC 1444: cal BC 1126], 1 2σ: [cal BC 1604: cal BC 959], 1
Chami-Tafarit	Ly-346	Arca Senilis313	3570 ± 120	1σ: [cal BC 2042: cal BC 1748], 0.93 2σ: [cal BC 2213: cal BC 1618], 0.98	1σ: [cal BC 1667: cal BC 1378], 1 2σ: [cal BC 1831: cal BC 1218], 1	1σ: [cal BC 1586: cal BC 1287], 1 2σ: [cal BC 1731: cal BC 1114], 1	1σ: [cal BC 1608: cal BC 1267], 1 2σ: [cal BC 1785: cal BC 1081], 1
Chami-Tafarit	Gif-1856	Chells, 15 a	3950 ± 80	1σ: [cal BC 2503: cal BC 2338], 0.72 2σ: [cal BC 2673: cal BC 2200], 0.99	1σ: [cal BC 2110: cal BC 1888], 1 2σ: [cal BC 2216: cal BC 1756], 1	1σ: [cal BC 2008: cal BC 1778], 1 2σ: [cal BC 2126: cal BC 1679], 1	1σ: [cal BC 2045: cal BC 1760], 1 2σ: [cal BC 2194: cal BC 1630], 1

Note: The calibrated ages chosen are those with the highest probability density.

BP, Before Present.

[a]Atmospheric calibration curve: Intcal13.^{14}C (Reimer *et al*., 2013).

[b]Marine calibration curve with world marine reservoir age: Marine13.^{14}C(Reimer *et al*., 2013).

[c]Marine calibration curve with estimated marine reservoir age: Marine13.^{14}C(Reimer *et al*., 2013).

[d]Marine calibration curve with estimated marine reservoir age: Marine20.^{14}C(Heaton *et al*., 2020).

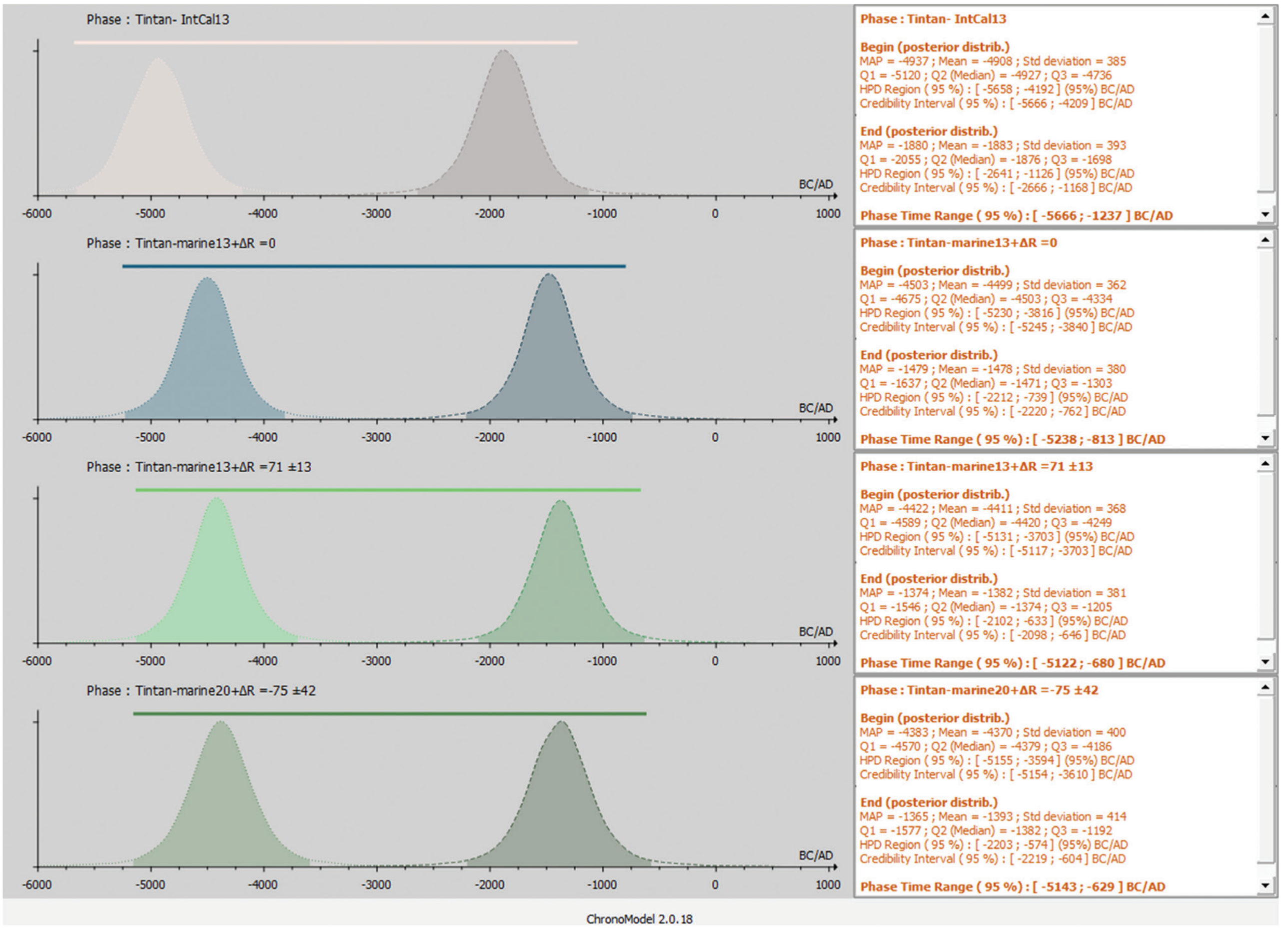

***Fig 4**. Calibration of the marine sample collected from Tintan site using chronomodel 2.0.18 with phase option.*

calibration curves (Intcal13, Marine13 + ΔR = 0 BP and Marine13 + ΔR = 71 ± 13 BP) and an ageing phase with Marine20 + ΔR = −75 ± 42 BP (Fig. 4). A comparison of the results of the calibration curves gives between Intcal13 and Marine13 with ΔR = 0 a 428-year rejuvenation difference of the start of occupation. This difference is 116 years between Marine13 with ΔR = 0 and Marine13 with ΔR = 71 ± 13 BP. The comparison between Marine13 with ΔR = 71 ± 13 BP and Marine20 with ΔR = −75 ± 42 BP marks an increase of 170 years, or 5666 years for Intcal13, 5238 years for Marine13 with ΔR = 0, 5122 years for Marine13 with ΔR = 71 ± 13 BP and 5143 years for Marine20 with reservoir effect. From the Intcal13 curve to the Marine13 curve, taking into account the reservoir effect, we have a decrease in the duration of occupancy of the site. However, with Marine20, we have an increase in site occupancy time compared to the previous two Marine13 curves. On the Marine13 base, without application of the Tintan Reservoir Effect, the period of occupancy ranges from 5666 BC to 629 BC with an interruption period of 1620 BC to 900 BC. This gives, with the local reservoir effect on Marine13, the intervals [5238 BC–680 BC].

Consequently, taking into account the ‘local reservoir’ (Marine13 or Marine20) rejuvenates the duration of Tintan’s occupation by 116 years and 184 years at its lower limits (813 BC and 680 BC). The marine20 calibration curve makes Tintan a site of the sixth millennium BC. This long human occupation of Tintan ended at the beginning of the Iron Age in West Africa. The lower limits or end of occupancy are, according to Marine13, 813 BC and 629 BC if the local reservoir effect is applied, i.e. a rejuvenation of more than a century and an ageing of 21 years with Marine20.

According to the Marine13 curve with ΔR = 0 (Table 3), the calibrated ages are the intervals [4658 BC–4338 BC] at 1σ and [4845 BC–4173 BC] at 2σ. This chronocultural periodisation of Tintan is confirmed by the intervals of Ly553 of ΔR = 71 ± 13 BP: [4588 BC–4261 BC] at 1σ and [4756 BC–4068 BC] at 2σ. This long human occupation

Table 3. *Calibration of marine samples collected at Tintan with the atmospheric curve, and the Marine curves (ΔR = 0 BP or ΔR = 71 ± 13 BP or ΔR = −75 ± 42 BP).*

Sample location	Sample code	Sample type	Age (BP)	Atmospheric calibration[a] (BC/AD)	Marine calibration[b] (BC/AD), ΔR = 0 BP	Marine calibration[c] (BC/AD) ΔR = 71 ± 13 BP	Marine calibration[d] (BC/AD) ΔR = −75 ± 42 BP
Tintan	Ly-460	Arca Senilis	3530 ± 130	1σ: [cal BC 2029: cal BC 1691], 1 2σ: [cal BC 2205: cal BC 1528], 1	1σ: [cal BC 1624: cal BC 1302], 1 2σ: [cal BC 1799: cal BC 1125], 1	1σ: [cal BC 1539: cal BC 1212], 1 2σ: [cal BC 1695: cal BC 1025], 1	1σ: [cal BC 1387: cal BC 1038], 1 2σ: [cal BC 1528: cal BC 850], 1
Tintan	FC-1	Cymbium 3455	3570 ± 160	1σ: [cal BC 2138: cal BC 1735], 0.96 2σ: [cal BC 2348: cal BC 1511], 0.99	1σ: [cal BC 1719: cal BC 1318], 1 2σ: [cal BC 1924: cal BC 1105] 1	1σ: [cal BC 1626: cal BC 1225], 1 2σ: [cal BC 1841: cal BC 1015], 1	1σ: [cal BC 1457: cal BC 1042], 1 2σ: [cal BC 1653: cal BC 834], 1
Tintan	FC-2	ArcaSenilis 3780	3695 ± 80	1σ: [cal BC 2154: cal BC 1973], 0.84 2σ: [cal BC 2341: cal BC 1882], 1	1σ: [cal BC 2154: cal BC 1973], 0.84 2σ: [cal BC 2341: cal BC 1882], 1	1σ: [cal BC 1676: cal BC 1477], 1 2σ: [cal BC 1786: cal BC 1387], 1	1σ: [cal BC 1523: cal BC 1289], 1 2σ: [cal BC 1656: cal BC 1170], 1
Tintan	FC-3	Arca Senilis313	3805 ± 80	1σ: [cal BC 2349: cal BC 2136], 0.8 2σ: [cal BC 2470: cal BC 2030], 1	1σ: [cal BC 1900: cal BC 1689], 1 2σ: [cal BC 2019: cal BC 1597], 1	1σ: [cal BC 1826: cal BC 1608], 1 2σ: [cal BC 1920: cal BC 1501], 1	1σ: [cal BC 1660: cal BC 1425], 1 2σ: [cal BC 1793: cal BC 1303], 1
Tintan	FC-4	Arca Senilis	3850 ± 100	1σ: [cal BC 2466: cal BC 2199], 0.98 1σ: [cal BC 2574: cal BC 2028], 1	1σ: [cal BC 1997: cal BC 1727], 1 2σ: [cal BC 2135: cal BC 1602], 1	1σ: [cal BC 1894: cal BC 1635], 1 2σ: [cal BC 2028: cal BC 1503], 1	1σ: [cal BC 1736: cal BC 1455], 1 2σ: [cal BC 1890: cal BC 1324], 1
Tintan Péheur	Gif-485	Oysters	3930 ± 80	1σ: [cal BC 2494: cal BC 2296], 0.89 2σ: [cal BC 2630: cal BC 2196], 0.98	1σ: [cal BC 2095: cal BC 1868], 1 2σ: [cal BC 2190: cal BC 1739], 1	1σ: [cal BC 1974: cal BC 1749], 1 2σ: [cal BC 2106: cal BC 1658], 1	1σ: [cal BC 1823: cal BC 1566], 1 2σ: [cal BC 1943: cal BC 1454], 1
Tintan	FC-5	ArcaSenilis mound L	3960 ± 100	1σ: [cal BC 2583: cal BC 2292], 0.98 2σ: [cal BC 2706: cal BC 2196], 0.92	1σ: [cal BC 2146: cal BC 1871], 1 2σ: [cal BC 2291: cal BC 1729], 1	1σ: [cal BC 2038: cal BC 1757], 1 2σ: [cal BC 2189: cal BC 1643], 1	1σ: [cal BC 1884: cal BC 1590], 1 2σ: [cal BC 2026: cal BC 1449], 1
Tintan	FC-6	ArcaSenilis490 FF	3970 ± 200	1σ: [cal BC 2699: cal BC 2204], 0.89 2σ: [cal BC 2941: cal BC 1901], 0.99	1σ: [cal BC 2287: cal BC 1749], 1 2σ: [cal BC 2554: cal BC 1512], 1	1σ: [cal BC 2192: cal BC 1662], 1 2σ: [cal BC 2460: cal BC 1434], 1	1σ: [cal BC 2016: cal BC 1492], 1 2σ: [cal BC 2301: cal BC 1246], 1
Tintan	Ly-503	Cymbium	4270 ± 100	1σ: [cal BC 3023: cal BC 2848], 0.62 2σ: [cal BC 3116: cal BC 2575], 0.96	1σ: [cal BC 2565: cal BC 2284], 1 2σ: [cal BC 2730: cal BC 2137], 1	1σ: [cal BC 2466: cal BC 2191], 1 2σ: [cal BC 2600: cal BC 2032], 1	1σ: [cal BC 1457: cal BC 1042], 1 2σ: [cal BC 1653: cal BC 834], 1
Tintan	FC-7	Mound 0 512	4445 ± 160	1σ: [cal BC 3198: cal BC 2925], 0.66 2σ: [cal BC 3530: cal BC 2840], 0.93	1σ: [cal BC 2867: cal BC 2466], 1 2σ: [cal BC 3078: cal BC 2207], 1	1σ: [cal BC 2828: cal BC 2397], 1 2σ: [cal BC 2977: cal BC 2124], 1	1σ: [cal BC 2592: cal BC 2140], 1 2σ: [cal BC 2832: cal BC 1946], 1
Tintan	FC-8	ArcaSenilis mound 0	4570 ± 140	1σ: [cal BC 3384: cal BC 3091], 0.75 2σ: [cal BC 3538: cal BC 2924], 0.93	1σ: [cal BC 3002: cal BC 2617], 1 2σ: [cal BC 3246: cal BC 2464], 1	[cal BC 2897: cal BC 2544], 1 [cal BC 3103: cal BC 2331], 1	1σ: [cal BC 2747: cal BC 2345], 1 2σ: [cal BC 2902: cal BC 2137], 1
Tintan	FC-9	ArcaSenilis mound	4600 ± 200	1σ: [cal BC 3534: cal BC 3089], 0.88 2σ: [cal BC 3796: cal BC 2866], 0.99	1σ: [cal BC 3121: cal BC 2568], 1 2σ: [cal BC 3376: cal BC 2315], 1	1σ: [cal BC 3018: cal BC 2480], 1 2σ: [cal BC 3329: cal BC 2252], 1	1σ: [cal BC 2855: cal BC 2322], 1 2σ: [cal BC 3103: cal BC 2015], 1
Tintan	FC-10	ArcaSenilis mound 0	4860 ± 160	1σ: [cal BC 3800: cal BC 3499], 0.85 1σ: [cal BC 3996: cal BC 3327], 0.98	1σ: [cal BC 3121: cal BC 2568], 1 2σ: [cal BC 3376: cal BC 2315], 1	1σ: [cal BC 3315: cal BC 2914], 1 2σ: [cal BC 3518: cal BC 2692], 1	1σ: [cal BC 3129: cal BC 2673], 1 2σ: [cal BC 3338: cal BC 2482], 1
Tintan	FC-11	Cymbium377 B	5020 ± 160	1σ: [cal BC 3970: cal BC 3651], 1 2σ:cal BC 4181: cal BC 3514], 0.97	1σ: [cal BC 3624: cal BC 3243], 0.98 2σ: [cal BC 3748: cal BC 2963], 1	1σ: [cal BC 3511: cal BC 3096], 1 2σ: [cal BC 3646: cal BC 2896], 1	1σ: [cal BC 3317: cal BC 2907], 1 2σ: [cal BC 3515: cal BC 2686], 1
Tintan	FC-12	ArcaSenilis266 E	5320 ± 150	1σ: [cal BC 4270: cal BC 4033], 0.79 2σ: [cal BC 4452: cal BC 3893], 0.95	1σ: [cal BC 3927: cal BC 3609], 1 2σ: [cal BC 4050: cal BC 3371], 1	1σ: [cal BC 3839: cal BC 3498], 1 2σ: [cal BC 3984: cal BC 3331], 1	1σ: [cal BC 3648: cal BC 3288], 1 2σ: [cal BC 3819: cal BC 3045], 1
Tintan	FC-13	ArcaSenilis central point	5520 ± 100	1σ: [cal BC 4462: cal BC 4311], 0.82 2σ: [cal BC 4559: cal BC 4220], 0.91	1σ: [cal BC 4058: cal BC 3802], 1 2σ: [cal BC 4213: cal BC 3724], 1	1σ: [cal BC 3976: cal BC 3750], 1 2σ: [cal BC 4106: cal BC 3641], 1	1σ: [cal BC 3803: cal BC 3541], 1 2σ: [cal BC 3947: cal BC 3429], 1

(*Continued*)

Table 3. *Continued*

Sample location	Sample code	Sample type	Age (BP)	Atmospheric calibration[a] (BC/AD)	Marine calibration[b] (BC/AD), ΔR = 0 BP	Marine calibration[c] (BC/AD) ΔR = 71 ± 13 BP	Marine calibration[d] (BC/AD) ΔR = −75 ± 42 BP
Tintan	FC-14	ArcaSenilis 377 A	5670 ± 300	1σ: [cal BC 4857: cal BC 4230], 0.94 2σ: [cal BC 5229: cal BC 3937], 0.98	1σ: [cal BC 4433: cal BC 3782], 1 2σ: [cal BC 4802: cal BC 3473], 1	1σ: [cal BC 4343: cal BC 3700], 1 2σ: [cal BC 4694: cal BC 3365], 1	1σ: [cal BC 4187: cal BC 3522], 1 2σ: [cal BC 4500: cal BC 3136], 1
Tintan Pécheur	Ly-553	Shells TAPES, 717	6020 ± 150	1σ: [cal BC 5074: cal BC 4724], 0.93 2σ: [cal BC 5301: cal BC 4581], 0.99	1σ: [cal BC 4658: cal BC 4338], 1 2σ: [cal BC 4845: cal BC 4173], 1	1σ: [cal BC 4588: cal BC 4261], 1 2σ: [cal BC 4756: cal BC 4068], 1	1σ: [cal BC 4384: cal BC 4034], 1 2σ: [cal BC 4581: cal BC 3865], 1

Note: The calibrated ages chosen are those with the highest probability density.

BP, Before Present.

[a]Atmospheric calibration curve: Intcal13.^{14}C (Reimer *et al.*, 2013).

[b]Marine calibration curve with world marine reservoir age: Marine13.^{14}C (Reimer *et al.*, 2013).

[c]Marine calibration curve with estimated marine reservoir age: Marine13.^{14}C (Reimer *et al.*, 2013).

[d]Marine calibration curve with estimated marine reservoir age: Marine20.^{14}C (Heaton *et al.*, 2020).

of Tintan ended at the beginning of the Iron Age in West Africa. This chronology (second–third millennium) is confirmed by ΔR = 0, [624 BC–1302 BC] at 1σ and [1799 BC–1125 BC] at 2σ and ΔR = 71 ± 13 BP with intervals [539 BC–1212 BC].

3.4. Comparison of Archaeological Sites

We use the Marine20 calibration curve for each site in case the reservoir effect is not applied (ΔR = 0) and in case it is applied (ΔR ≠ 0).

3.4.1. Comments 4

The use of the Marine20 calibration curve taking into account the reservoir effect shows a rejuvenation of the beginnings of human occupations (a gap of 10 BC) but also of the ends of occupations (a gap of 92 AD) for the Khant site On the other hand, for the two sites of Mauritania, taking into account the reservoir effect causes ageing of the occupation phases. (Fig. 5). In a phylogenetic approach, the phylogenetic data (cymbium, Arca senilis, oyster) dated confirm that the end of the occupation of Tintan coincides with the beginning of the occupation of the 'populations' of Chami. Tintan is the oldest of the three stations studied. If ΔR = 0, occupation begins in 5238 BC, followed by a period of hiatus [1268 BC–1870 BC], 578 years before the start of the Khant stand (4660 BC), based on samples collected. The long period of abandonment lasted less than a millennium (860 BC). The reoccupation of the site, starting from 500 BC, is contemporary, in its upper margins, of the Chami station whose human occupation dynamic covers the phase [2481 BC–1500 BC]. Thus, the beginning of the occupation in Chami, by the dating obtained, suggests a transition or migration of the populations from Tintan to Chami. Indeed, the abandonment of Tintan coincides with the displacement of isohyetes, or aridity, from north to south of Mauritania, corresponding to the marine transgression of 2200 BC. Long period of climatic drying involves migration of populations around the Tintan Peninsula.

This period of aridity will be followed by a probable recovery of the isohyetes, as the region repopulates [2000 BC–685 BC] until the beginning of the first phase of the age of metals. Moreover, the contemporaneity between Tintan and Khant goes from the fifth to the fourth millennium BC. The period of interruption in Khant is long [3200 BC–400 BC]. This is likely the result of the sample collection context (Tables 1 and 3). Thus, in its upper layers, Khant is contemporary with Chami, if ΔR = 0, during the phase of protohistoric occupation. This raises the question of the contextualisation of the samples and the probable reoccupation of Khant. Then, the phase of interruption of Tintan, with the aridity of the region linked to the transgression of Nouakchottien. The 'revitalisation of the people' of

***Fig 5**. Calibration by Marine20 curve of the marine sample collected from the 3 sites (Chami, Tintan, Khant) using chronomodel 2.0.18 with phase option.*

Tintan [2880 BC–629 BC] is clear evidence of its precedence on other sites whose dates obtained vary from 1100 BC to 118 BC for Khant and from 1500 BC to 462 BC for Chami. Thus, taking into account the reservoir effect with marine20 does not affect the calibration of the marine samples, even if there is a «longer life expectancy» of the samples, but confirms the rejuvenation of the dates of a few centuries. Therefore, the application of the 'reservoir effect correction' shows that Chami is more historical than Tintan.

4. Conclusion

This study shows the need and importance of applying reservoir age to the chronology of Senegalese-Mauritanian coastal sites. In general, the application of the marine reservoir effect to the different Senegalese-Mauritanian sites shows a rejuvenation of the samples if Marine13 is used. However the calibration curves of Marine20 of the chronological phases cause the ageing of the samples of Chami and Tintan.

From the simplified synthesis, the interpretations made on the samples taken, taking into account the chronological phases of the local reservoir age (Marine13 and Marine20), confirm that the dynamics of the human settlement at Khant is a process that extends from prehistory to history from the fifth millennium BC (4598 BC for Marine13 with $\Delta R = 71 \pm 13$ BP and 4560 BC for Marine20 with $\Delta R = 27 \pm 56$ BP) at the beginning of history or even beyond (medieval) with prolonged interruption phases. As a result, the dates are relatively young.

By using Marine13 with $\Delta R = 71 \pm 13$ BP, the Tintan site is rejuvenated (5238 BC to 5122 BC) despite this there remains an older site than Khant. Tintan is the oldest of the Neolithic sites studied (5143 BC with Marine20), despite a phase of abandonment. The end of its occupation was at the beginning of the early age of iron metallurgy in West Africa (629 BC, Marine20). The displacement of the occupation dynamics of the Mauritanian coastline from Tintan to Chami, after the transgression of the Nouakchottians led the populations towards the southwest of Mauritania. The settlement of Chami is attested to in the third millennium BC (from 2378 BC with Marine13, to 2466 BC with Marine20). It ends in medieval times (from the 5th to the 15th century AD), therefore, the passage from Marine13 $\Delta R = 71 \pm 13$ BP to Marine20, $\Delta R = 75 \pm 42$ BP, shows an ageing of the samples collected. This raises the problem of reviewing the dates obtained.

In turn, in its lower limits, Chami is contemporary with Khant. In filigree, the 'markers' taken and dated provide information on the duration of human occupation of the three sites studied. Thus, if $\Delta R = 0$, the human occupation in Khant goes from the fifth to the third millennium with periods of interruption. In Tintan, it extends from the fifth to the second millennium. During the terminal phase of this occupation, the Chami site was populated from the third millennium to the second century (Table 2). On the other hand, if the reservoir effect is taken into account, it does not alter the prehistoric periods too much despite the differences in methods applied. Khant and Tintan are contemporaries on long chronocultural sequences (from 4598 BC to 238 BC with $\Delta R = 71 \pm 13$ BP and from 3770 BC to 680 BC, with $\Delta R = 75 \pm 42$ BP) even if the occupation of the site of Khant continues until the beginning of the protohistory. The calibration by Marine20 gives Tintan a 21-year increase in Tintan samples. Moreover, in its terminal phase, Khant (third millennium–second century AD) is contemporary with Chami, whose occupation is a priori linked to the taphonomic mastery of the populations.

Indeed, the passage from Tintan to Chami occurred between 3600 BC and 2378 BC, therefore with the Marine20 calibration, the occupation of the Chami deposit is in 2466 BC or an 'extended life expectancy' of 88 years.

Acknowledgements

This work was supported by the Radiocarbon laboratory of IFAN Cheikh Anta DiopofDakar (Cheikh Anta Diop University). We express our thanks to all the to the team of the archeology laboratory IFAN Cheikh Anta Diop de Dakar for having made available the archaeological data used. In particular, we would like to thank Mr Nicolas Serge (mapmaker) from Geography Laboratory of IFAN for the important contributions made to this research article.

Supplementary Information

Supplementary information are available online at: DOI: 10.2478/geochr-2021-0002

References

Carbonnel JP, 1979. Structure et paléoenvironnement d'un site néolithique Mauritanien: ksar Jmel (Tintan). (Structure and palaeoenvironment of a Mauritanian Neolithic site; ksar Jmel (Tintan)). *Notes Africaines* 137: 1–6.

Delibrias G, et Evin J,1980. Sommaire des datations ^{14}C en France, dates parues de 1974 à 1978. (Table of Contents of ^{14}C Dating in France, dates published from 1974 to 1978). *Bulletin de la société Prehistorique de France* L77: 215–224.

Druffel ERM and Griffin S, 1993. Variability of surface ocean radiocarbon and stable isotopes in the southwestern Pacific. *Journal of Geophysical Research* 104(C10): 23607–23613.

Dunbar RB and Cole JE, 1996. *Annual Records of Tropical Systems (ARTS). Recommendations for Research*. Department of Geological and Environmental Sciences Stanford University, Stanford CA 94305-2115, USA.

Farida M, 2013. Apport de l'imagrie médicale et tridimensionnelle à l'étude des restes humains datant de l'holocène ancient (Sahara Malien et Mauritanien), analyse craniologique comparative. Thèse de Doctorat de l'université d'Aix-Marseille, 261pages (Contribution of medical and three-dimensional imagery to the study of human remains dating from the ancient holocene (Malian Sahara and Mauritanian), comparative craniological analysis. Doctoral thesis of the University of Aix-Marseille, 261pages).

Goodfriend AG and Flessa KW, 1997. Radiocarbon reservoir ages in the Gulf of California: roles of upwelling and flow from the Colorado River. *Radiocarbon* 39(2): 139–148.

Heaton TJ, Köhler P, Butzin M, Bard E, Reimer RW, Austin WEN, Ramsey CB, Grootes PM, Hughen KA, Kromer B, Reimer PJ, Adkins J, Burke A, Cook MS, Olsen J and Skinner LC, 2020. Marine20 – The Marine Radiocarbon age calibration curve (0–55,000 Cal BP). *Radiocarbon* 62(4): 779–820.

Hebrard L, 1978. Contribution a l'étude géologique du Quaternaire du littoral mauritanien entre Nouakchott et Nouadhibou, 18o21'latitude Nord. Participation a l'étude des désertifications du sahara. Thèse de Doctorat de l'université Claude Bernard, Lyon.212 pages (Contribution to the geological survey of the Mauritanian Coastal Quaternary between Nouakchott and Nouadhibou, 18°21'north latitude. Doctoral thesis of Claude Bernard University, Lyon.212 pages).

Láiz I, Sangra P and Pelegry JL, 2000. Variabilidad estacional del borde oriental del Giro subtropical del Atlantico. *Notes.simposio sobre a Margem Iberia Atlantico*: 159–160 (Seasonal variability of the eastern edge of the subtropical Gyre of Atlantico. Notes. symposium on Margem Iberia Atlantico: 159–160).

Lanos P and Philippe A, 2015. Hierarchical Bayesian modeling for combining dates in archaeological context. hal-01162404v2.

Mbow MA, 1987. *Les Amas coquilliers du Delta du Sénégal: Étude, Ethnoarchéologique* (The Shellfish Clusters of the Senegal Delta: Study, Ethnoarcheology). Thèse de doctorat non publiée, Université Paris I, Panthéon-Sorbonne: 366 pp.

Ndeye M, 2008. Marine reservoir ages in northern Senegal and Mauritania coastal waters. *Radiocarbon* 50(2): 281–288.

Packard,1999.Quanta Smart for the tricarb liquid scintillation analyser Reference Manuel .Publication No 1694215 Rev.A, Print in USA.

Pelegrí JL, Marrero-Diaz A and Ratsimandresy AW, 2006. Nutrient irrigation of the north Atlantic. *Progress in oceanographic* 70(2–4): 366–406.

Petit-Maire N, 1979. Le Sahara atlantique à l'holocène peuplement et ecologie (The Atlantic Sahara to Holocene Settlement and Ecology). *Mémoires du centre de recherches anthropologiques, préhistoriques et ethnographiques* vol. XXVIII

Ravisé A, 1970. Industries en os de la region de St-Louis (Bone industries in the St-Louis region). *Notes Africaines* 128: 98–102.

Ravisé A, Thilmans G and Marius C, 1975. Etude d'un squelette néolitique de la region de St-Louis. (Study of a neo-political skeleton in the St-Louis region). *Bulletin IFAN* 37: 687–701.

Reimer PJ, Bard E, Bayliss A, Beck JW, Blackwell PG, Ramsey CB, Buck CE, Cheng H, Edwards RL, Friedrich M, Grootes PM, Guilderson TP, Haflidason H,Hajdas I, Hatté C, Heaton TJ, Hoffmann DL, Hogg AG,Hughen KA,Kaiser KF, Kromer B, Manning SW, Niu M, Reimer RW,Richards DA, Scott EM, Southon JR, Staff RA, Turney CSM and van der Plicht J, 2013. IntCal13 and Marine13 Radiocarbon age calibration curves 0–50,000 years cal BP. *Radiocarbon* 55(4): 1869–1887.

Siani G, Paterne M, Arnold M, Bard E, Metivier B, Tisnerat N and Bassino F, 2000. Radiocarbon reservoir ages in the Mediterranean sea and black sea. *Radiocarbon* 42(2): 271–280.

Soares AMM, Martins JMM and Cardoso JL, 2011. Marine reservoir effect of coastal waters off Cape Verde Archipelago. *Radiocarbon* 53(2): 289–296; DOI: 10.1017/S0033822200056551.

Southon J, Kashgaran M, Fontugne M, Metivier B and Yimm WW-S, 2002. Marine reservoir corrections for the Indian ocean and the southeast Asia. *Radiocarbon* 44(1): 167–189.

Stuiver M and Polach H, 1977. Reporting of ^{14}C data. *Radiocarbon* 19(3): 355–363.

Stuiver M, Reimer PJ and Braziunas TF, 1986. High precision radiocarbon age calibration for terrestial and marine samples. *Radiocarbon* 40(3): 1127–1151.

Stuiver M and Braziunas TF, 1993. Modeling atmospheric 14 C influences and 14 C ages of Marine samples to 10,000 BC. Radiocarbon 35(1): 137–189.

Stuiver M, Reimer PJ and Braziunas TF, 2013. High-precision radiocarbon age calibration for terrestrial and marine samples. *Radiocarbon* 40(3), 1998, 1127–1151.

Stuiver M, Reimer PJ and Reimer RW, 2020. CALIB 8.2 [WWW program]. WEB site <http://calib.org>. Accessed 2020 July 13.

Vernet R, 1993. Prehistoire de la Mauritanie. Nouakchott (Prehistory of Mauritania.Nouakchott) CCF, Nouakchott-Sépia.

Vernet R, 1998. Le sahara et le sahel, paléoenvironnments et occupation humaine a la fin du pléistocéne et a l'holocéne (The Sahara and the Sahel, paleo-environments and human occupation at the end of the pleistocene and the holocene). [In:] *Inventaire des datations ^{14}C*. 2^{e} édition: jusqu'en 1997.

Vernet R, 2004. *Peuplement des régions littorales et occidentales: le « Projet Khant »* (Settlement of coastal and western regions: the «Khant Project»). [In:] Archéologies, vingt ans de recherches françaises dans le monde, Maisonneuve et Larose/ADPF/ERC.

Vernet R and Tous P, 2004. Les amas coquilliers de Mauritanie occidentale et leur contexte paléoenvironnemental (VIIe-IIe millénaires BP). (Shellfish clusters in Western Mauritania and their palaeoenvironmental context (7th-3rd millennia BP)). *Préhistoire et Anthropologie Méditerranéennes* 13: 1–15.

Vernet R, Galin A, Saliège JF and Tous P, 2004. Chronologie isotopique de l'occupation humaine sur le rivage du maximum nouakchottien (Mauritanie atlantique). (Isotopic chronology of human occupation on the shore of the nouakchottian maximum (Atlantic Mauritania)) *Al-Wasît, Revue de l'Institut Mauritanien de Recherche Scientifique* 8: 15–35.

Wooster WS, Bakun A and Mclain DR, 1976. The seasonal upwelling cycle along the eastern boundary of the north Atlantic. *Journal of Marine Research* 34(2): 131–141.